Original Research

ONECUT2 which is targeted by hsa-miR-15a-5p enhances stemness maintenance of gastric cancer stem cells

Chen Shen[1], Junfeng Wang[1], Zhihua Xu[2], Liping Zhang[3], Wen Gu[2] and Xiaojun Zhou[2]

[1]Department of General Surgery, The 904th Hospital of PLA Joint Logistics Support Force, Suzhou 215007, PR China; [2]Department of General Surgery, The First Affiliated Hospital of Soochow University, Suzhou 215006, PR China; [3]Department of Gastroenterology, The Affiliated Suzhou Hospital of Nanjing Medical University, Suzhou 215000, PR China

Corresponding authors: XJ Zhou. Email: shmilymessi@163.com; W Gu. Email: 13771746471@163.com

Impact statement

Due to our limited knowledge with regard to the pathogenesis of gastric cancer, the five-year overall survival of gastric cancer patients still remains perishing. In this paper, we demonstrated that hsa-miR-15a-5p and ONECUT2 represent good candidates for diagnosis and prognosis in gastric cancer. ONECUT2 is related to cancer stage, metastasis, and grade, and its expression is inversely proportional to the differentiation degree of gastric adenocarcinoma. Besides, compared with parental MKN45, the expression levels of hsa-miR-15a-5p in CD133+/CD44+ MKN45 was down-regulated, while ONECUT2 was up-regulated. Hsa-miR-15a-5p regulates the stemness maintenance, epithelial–mesenchymal transition, and chemosensitivity of CD133+/CD44+ MKN45 through regulation of its target gene ONECUT2. Hsa-miR-15a-5p inhibits G0 phase block of CD133+/CD44+ MKN45 by regulating ONECUT2/β-catenin signaling pathway. However, this study provides the potential implication of biomarkers hsa-miR-15a-5p and ONECUT2 in the pathogenesis of gastric cancer.

Abstract

Gastric cancer is the third dominating cause of cancer-associated death. MiroRNAs are potential clinical tools for cancer diagnosis and therapy. In this project, we demonstrated significant overexpression of ONECUT2 and down-regulation of hsa-miR-15a-5p in gastric cancer via bioinformatics analysis and *in vitro* assays. Meanwhile, ONECUT2 expression is related to clinical prognosis in gastric cancer and inversely proportional to the differentiation degree of gastric adenocarcinoma according to immunohistochemistry results. Then, we separated CD133+/CD44+ MKN45 by flow cytometry and found that, compared with parental MKN45, CD133+/CD44+ MKN45 gastric cancer stem cells (GCSCs) had higher levels of ONECUT2 and lower levels of hsa-miR-15a-5p. In addition, we applied both *in vivo* and *ex vivo* assays to demonstrate hsa-miR-15a-5p regulates the stemness maintenance, epithelial–mesenchymal transition, and chemosensitivity of GCSCs through targeting ONECUT2. Also, hsa-miR-15a-5p inhibits G0 phase block of GCSCs by regulating ONECUT2/β-catenin signaling pathway. However, this study has provided novel perspective into the dynamic control of cancer stem cells for advanced gastric cancer treatment.

Keywords: Gastric cancer, CD133+/CD44+, hsa-miR-15a-5p, ONECUT2, stemness

***Experimental Biology and Medicine* 2021; 246: 2645–2659. DOI: 10.1177/15353702211038496**

Introduction

Gastric cancer (GC) ranks the fifth in the incidence rate and the third in the mortality among all types of cancers.[1,2] In normal tissues, a small number of cell populations called stem cells (SCs) are able to self-renew and differentiate to form complete tissues. Cancer stem cells (CSCs) have been well recognized in many solid malignancies, including GC, and possess significant clinical implications. CSCs have been identified as the driving force of tumorigenesis and the origins and seeds of metastases.[3] Targeting CSCs might be potential in preventing the recurrence, drug resistance, and metastasis.

In the tumor microenvironment, cancer cells acquire the migratory phenotype and stem cell characteristics through epithelial–mesenchymal transition (EMT). EMT inhibits the intercellular adhesion mediated by E-cadherin to make epithelial cells acquire a mesenchymal phenotype and promote cancer cell infiltration. EMT and stemness properties respectively or synergistically endow chemotherapy resistance to cancer cells.[4,5]

ONECUT is a highly conserved family of transcription factors and plays a critical role in organ development.[6] ONCUT2 expression could be detected in the developing pancreas, liver, nervous system, and intestinal endoderm.[7] The literature has shown that ONECUT2 is overexpressed among a variety of cancers such as bladder cancer, prostate cancer, ovarian cancer, colorectal cancer, and liver cancer.[8–14] These studies demonstrated that ONECUT2 can promote the proliferation, invasion, and metastasis of cancer cells. However, the role of ONECUT2 in GC is still unclear. Shen *et al.* revealed that ONECUT2 regulates CSC phenotype and the levels of stemness-related genes in breast cancer. ONECUT2 could enhance the self-renewal ability of non-small cell lung cancer cells.[15] Besides, ONECUT2 enhances CSC phenotype after chemotherapy in breast cancer.[16] Thus, it is proposed that ONECUT2 might be engaged in mediating the stemness of cancer cells.

MicroRNA (miRNA) is small non-coding RNA composed of 19–24 nucleotides. It acts as a post-transcriptional gene regulator via binding to the certain sequence in the 3′-untranslated region of the target gene to degrade mRNA or inhibit its translation into functional protein.[17] MiRNA is closely linked to the clinical prognosis, resistance to chemotherapy and radiotherapy, and recurrence in cancers. miRNA is thought to regulate CSC phenotype through sundry signaling pathways. A variety of abnormally expressed miRNAs have been found in GC. They may become a new type of markers, which are of great significance in the diagnosis and treatment of GC.

In this research, we demonstrated significant down-regulation of hsa-miR-15a-5p and up-regulation of ONECUT2 in GC samples. Then, we separated CD133+/CD44+ GC cell line MKN45 as gastric cancer stem cells (GCSCs). Then, we applied both *in vivo* and *ex vivo* assays to demonstrate whether hsa-miR-15a-5p regulates the stemness, EMT, and drug sensitivity of GCSCs through the regulation of its target gene ONECUT2. However, this project provides new insights into the potential implication of hsa-miR-15a-5p and its target ONECUT2 in the pathogenesis of GC.

Materials and methods

Cell culture, reagents, and transfection

Human gastric adenocarcinoma cell lines HGC-27, AGS, SGC-7901, MKN45, and normal human gastric mucosal epithelial cell line GES-1 are cultivated in RPMI-1640 medium (Gibco, CA, USA) containing 10% fetal bovine serum (16000-044, Gibco, CA, USA), 100 U/mL penicillin, and 100 U/mL streptomycin. CD133+/CD44+ MKN45 were cultured in DMEM/F12 (Gibco, CA, USA) supplemented with 20 ng/mL epidermal growth factor (EGF), 10 ng/mL basic fibroblast growth factor (bFGF) (Peprotech, NJ, USA), 2% B27, and 5 μg/mL insulin (Sigma-Aldrich, MO, USA), while CD133-/CD44- MKN45 in Dulbecco's Modified Eagle's Medium/Nutrient Mixture F-12 (DMEM/F12) containing 10% fetal bovine serum. ONECUT2 (NM_004852) overexpression vector (OE) construction: Primers were designed based on pEGFP-n1 vector and target fragment (F: GGAATTCCATGAAGG CTGCCTACACCGCCTAT; R: CCTCGAGGGTGTCTGGT TCTAAGAGATTAATTT). After routinely digested, cells are cultured in a six-well plate. When cell density reaches about 70%, plasmids are transfected according to the instruction of Lipofectamine™ 3000 (Thermo Fisher Scientific, MA, USA).

Bioinformatics analysis

We utilized LIMMA R package to conduct differential expression analysis. $|\log2\text{Fold Change}| > 1$ and adjust $P < 0.05$ was set as the thresholds for differentially expressed genes (DEGs). ONECUT2 and DEGs whose absLogFC value ranked top 10 were shown. Gene Expression Profiling Interactive Analysis (GEPIA) (http://gepia.cancer-pku.cn/) analyzed the correlation between ONECUT2 expression levels and clinical outcomes of stomach adenocarcinoma (STAD) patients.[18] UALCAN cancer database (http://ualcan.path.uab.edu/) analyzed the correlation between ONECUT2 expression and STAD stage, grade, and metastasis.[19] MiRNA target gene prediction websites (PITA, RNA22, miRmap, microT, miRanda, PicTar, TargetScan) predicted ONECUT2-targeted miRNAs. In order to screen the signaling pathways regulated by ONECUT2 in GC, patients in the cancer genome atlas (TCGA) Database were divided into ONECUT2-high and ONECUT2-low expression groups, separately. When performing ONECUT2 grouping, we first sorted the expression of ONECUT2 from high to low, and then used the top 25% as the high-expression group, and the last 25% as the low-expression group. This is the quartile analysis method. The optimal cut-off 9.884 was applied to stratify the high versus low groups. Then, gene set enrichment analysis (GESA) analyzed ONECUT2-enriched signaling pathway (nominal P value < 0.05). Enrichr database (https://maayanlab.cloud/Enrichr/) analyzed kyoto encyclopedia of genes and genomes (KEGG) pathway enrichment for DEGs.[20]

Real-time RT-PCR

Real-time reverse transcription-polymerase chain reaction (RT-PCR) assay followed the instruction of Hieff UNICON quantitative real-time polymerase chain reaction (qPCR) SYBR Green Master Mix (Yeasen, Shanghai, China) and TransScript Green miRNA Two-Step qRT-PCR SuperMix (Transgene Biotech, Beijing, China). GAPDH was generally used as a housekeeping gene for mRNA and U6 was for miRNA. Their efficiencies have been compared before analysis. In addition, before formal qPCR assays, we have verified the specificity of all primers; moreover, we have also verified the overexpression efficiency of ONECUT2 OE and

Table 1. Primers in the real-time PCR.

Gene	Sequence (5′→3′)
Vimentin	F:GAAGAGAACTTTGCCGTTG
	R:GAAGGTGACGAGCCATTT
E-cadherin	F:GGTTGATCCTGGCTTTGTT
	R:GCCCTGTTGTCCTTCTTTT
Sox2	F:CGAACCATCTCTGTGGTCT
	R:GTGTCAACCTGCATGGC
CD44	F:AGTCCCTGGATCACCGA
	R:CCTCTTGGTTGCTGTCTCA
KLF4	F:AGGAGCCCAGCCAGAAA
	R:TCCAGTCACAGACCCCATC
ONECUT2	F:CCTTTTCCTTGGAGACACA
	R:CCCATGACCTGCCTTTT
GAPDH	F:CCTTCCGTGTCCCCACT
	R:GCCTGCTTCACCACCTTC
hsa-miR-15a-5p	UAGCAGCACAUAAUGGUUUGUG
Nanog	F:CCCTGATTCTTCCACCAGT
	R:CGGGACCTTGTCTTCCTT
OCT4	F:GCAAGCCCTCATTTCACC
	R:CCATCACCTCCACCACCT
N-cadherin	F:AGCCTGAGCAACAGCGA
	R:ACAGCCCGCAGACTTCTT

hsa-miR-15a-5p mimics by qPCR. The sequences of qPCR primers are listed in Table 1.

Western blot

Total proteins were separated on a 10% SDS-PAGE gel, and transferred onto PVDF membranes (Bio-Rad Laboratories Inc., CA, USA). After blocked with 5% BSA-TBST for 2 h, membranes were incubated with primary antibodies overnight such as ONECUT2 (ab247128, Abcam, Cambridge, UK), CD44 (DF6392, 1:1000, Affinity Biosciences), KLF4 (B-8, sc-393462, 1:1000, Santa Cluz, CA, USA), OCT4 (CY5781, 1:500, Abways Technology Inc., Shanghai, China), E-cadherin (67A4, sc-21791, 1:1000, Santa Cluz), N-cadherin (CY5015, 1:1000, Abways), Vimentin (V9, sc-6260, 1:1000, Santa Cluz), CyclinD1(AF0931, 1:1000, Affinity Biosciences), C-myc (CY1463, 1:1000, Abways), Survivin (CY5070, 1:1000, Abways), β-catenin (CY3523, 1:2000, Abways) and GAPDH (AB0036, 1:3000, Abways). The results were detected with horseradish peroxidase (HRP) chemiluminescence detection reagent (Tiangen Biotech, Beijing, China). Image J software (Rawak Software Inc., Stuttgart, Germany) was used for semi-quantitative analysis.

Besides, CD44, KLF4, OCT4 are stemness-related proteins used for CSC identification; E-cadherin, N-cadherin, Vimentin are EMT-related proteins used for exploring whether hsa-miR-15a-5p could regulate EMT of GCSCs by targeting ONECUT2; CyclinD1, C-myc, Survivin, β-catenin are key molecules of Wnt signaling pathway used for exploring whether hsa-miR-15a-5p could inhibit the block of G0 phase by regulating Wnt/β-catenin pathway.

Immunohistochemistry

Thirty cases of human GC and paired adjacent normal tissues were collected by The First Affiliated Hospital of Soochow University. GC tissue contains eight cases of highly, moderately, and poorly differentiated samples. All clinical samples were both approved by patients and the ethics committee of the 904th Hospital of Joint Logistics Support Force of PLA. ONECUT2 anti-human antibody (Affinity Biosciences, OH, USA) was diluted at a ratio of 1:150. Staining results were examined under microscope with 20× objective. Semi-quantitative analysis was conducted by Image-Pro Plus 6.0 (Rawak Software Inc., Stuttgart, Germany).

Flow cytometry sorting CD133+/CD44+ MKN45

Cells were washed by phosphate buffered saline (PBS) buffer after routine digestion, then incubated with 2.5% BSA at RT for 30 min; CD44-FITC and CD133-PE (eBioscience, CA, USA) were diluted with PBS at a ratio of 1:100 and incubated the cells at RT for 1 h; then cells were washed and resuspended in 400 μL PBS. Flow cytometry (Becton, Dickinson and Company, NJ, USA) was applied to sorting CD133+/CD44+ MKN45 and CD133-/CD44- MKN45.

Colony formation assay

CD133+/CD44+ MKN45, CD133-/CD44- MKN45, and parental MKN45 were cultured in a six-well plate (5×10^3 cells/well) with DMEM/F12 containing 5% FBS. Photos of the plate were taken by camera on the 14th day.

MTT assay

CD133+/CD44+ MKN45, CD133-/CD44- MKN45, and parental MKN45 were cultured in a 96-well plate with a density of 5×10^3 cells/well. After 12 h, 5-FU, cisplatin (DDP), and vincristine (VCR) of five concentration (6.25, 12.5, 25, 50, 100 μg/mL) were added and cells were incubated for 48 h in the dark. Then, we follow the methods described in the previous study[21] and apply 3-(4,5)-dimethylthiahiazo (-z-y1)-3,5-di-phenytetrazoliumromide (M2128, Sigma-Aldrich, MO, USA) to detect the cell viability.

Luciferase reporter assay

Wild-type and mutant 3′ UTR of ONECUT2 were inserted into PGL3-promoter vector. CD133+/CD44+ MKN45 were transfected with 800 ng pGL3-ONECUT2-WT or pGL3-ONECUT2-Mut, pcDNA-miR-15a-5p, and 40 ng pRL-TK vectors. Luciferase activity was measured 48 h later using Dual Luciferase Reporter Gene Assay Kit (Beyotime Biotechnology, Shanghai, China). Firefly luciferase activities were normalized to Renilla luciferase activities.

Sphere formation assay

CD133+/CD44+ MKN45 was digested and adjusted to 1000 cells/well in a 24-well plate. After two weeks, the number of spheres whose diameter are over 50 μm was counted and the average diameter of spheres in eight random fields was measured.

In vivo limiting dilution

Forty-five six-week-old male BALB/c nude mice were purchased from Shanghai Jiesijie Experimental Animal Co., Ltd. The animal operation complies with the guidelines for the care and use of laboratory animals authorized by the Ministry of Science and Technology of the People's Republic of China, and was approved by the Ethics Committee of Suzhou TCM Hospital Affiliated to Nanjing University of Chinese Medicine. Mice were randomly divided into nine groups (five mice per group). Groups: miRNA negative control (2×10^3); hsa-miR-15a-5p mimics (2×10^3); hsa-miR-15a-5p mimics+pEGFP_E2-2 (2×10^3); miRNA negative control (2×10^4); hsa-miR-15a-5p mimics (2×10^4); hsa-miR-15a-5p mimics+pEGFP_E2-2 (2×10^4); miRNA negative control (2×10^5); hsa-miR-15a-5p mimics (2×10^5); hsa-miR-15a-5p mimics+pEGFP_E2-2 (2×10^5). Four weeks later, the tumor formation of the mice was observed and photographed.

In vitro limiting dilution

CD133+/CD44+ MKN45 were diluted into 1000, 500, 250, 125, 60 cells/well in a low attach 96-well plate (Corning, NY, USA). Each group has 24 replicates. After two weeks, we counted the sphere numbers. Extreme Limiting Dilution Analysis (http://bioinf.wehi.edu.au/software/elda/) was applied to analyze the initiating frequency of CSCs.

Cell cycle analysis

CD133+/CD44+ MKN45 were routinely digested and fixed with 70% pre-cooled ethanol at 4°C overnight. Then, the cells were stained with propionium iodide staining solution (Beyotime Biotech, Shanghai, China). The DNA content was measured by flow cytometry and Flowjo 7.6 (Becton, Dickinson and Company, NJ, USA).

Statistical analysis

The data were analyzed by Graphpad Prism 8.0 (GraphPad Software Inc., CA, USA), and shown as mean ± standard deviation (SD). Results comparing two groups were analyzed by Student's *t* test. *P* value < 0.05 was regarded to be statistically significant.

Results

ONECUT2 is an oncogene in gastric cancer

We utilized LIMMA R package to conduct differential expression analysis of STAD samples and adjacent normal tissues in TCGA Database. After TCGA Database bioinformatics analysis, ONECUT2 and DEGs whose absLogFC ranked top 10 were exhibited in a histogram (Figure 1(a)). Then, our qPCR results showed that the expression of ONECUT2 in GC tissues was twice that in adjacent normal tissues ($P < 0.05$) (Figure 1(b)).

Subsequently, we clinically collected 30 cases of GC tissues and paired normal adjacent tissues. The results of qPCR and Western blot showed that compared with corresponding adjacent normal tissues, ONECUT2 was highly expressed in GC tissues ($P < 0.001$) (Figure 1(c) and (d)). Immunohistochemical results of our clinical samples showed that ONECUT2 was mainly concentrated in cytoplasmic and nuclear, and semi-quantitative analysis showed that it was overexpressed in GC tissues ($P < 0.01$) (Figure 1(e) and (f)). In addition, GEPIA (http://gepia.cancer-pku.cn/) was applied to assess the correlation between ONECUT2 expression and the survival of STAD patients. The bioinformatic analysis demonstrated that the lower the expression of ONECUT2, the longer the survival period of patients ($P < 0.05$) (Figure 1(g) and (h)).

ONECUT2 is inversely proportional to differentiation degree of gastric cancer tissue

UALCAN (http://ualcan.path.uab.edu/) was applied to analyze the correlation between ONECUT2 expression and STAD stage, grade, metastasis and the bioinformatics results demonstrated that the expression of ONECUT2 in GC tissues of different stages (Stages 1–4) was higher than that in adjacent normal tissues ($P < 0.05$) (Figure 2(a)). Compared with GC without lymph node metastasis, ONECUT2 expression was higher in GC with lymph node metastasis, and its expression increased with the increase of lymph node metastasis ($P < 0.05$) (Figure 2(b)). The expression of ONECUT2 in GC tissues of different grades (Grades 1–4) was higher than that in adjacent normal tissues ($P < 0.05$); compared with well differentiated (low grade) tissues, the expression of ONECUT2 in poorly differentiated (high grade) tissues is higher ($P < 0.001$), indicating ONECUT2 may be related to the grade of GC tissues, further suggesting ONECUT2 may regulate the stemness of GC cells (Figure 2(c)).

Next, we detected the expression of ONECUT2 in poorly differentiated, moderately differentiated, and well-differentiated adenocarcinoma via immunohistochemistry. The experimental results proved that the expression of ONECUT2 was inversely proportional to the differentiation degree of GC tissues (Figure 2(d) and (e)). Subsequently, we searched seven miRNA target gene prediction websites (PITA, RNA22, miRmap, microT, miRanda, PicTar, TargetScan) to predict miRNAs that regulate ONECUT2. The statistical results showed that six miRNA prediction websites indicate that hsa-miR-147a is the miRNA that targets ONCUT2, and five miRNA prediction websites indicate that hsa-miR-15a-5p, hsa-miR-27a-3p, hsa-miR-15b-5p, hsa-miR-27b-3p, hsa-miR-153-3p, hsa-miR-424-5p are miRNAs that target ONCUT2 (Figure 2(f)). Through literature search, we found that hsa-miR-15a-5p is related to GC and stemness. Therefore, we detected its expression in GC tissues and corresponding adjacent normal tissues by qPCR. The results proved that hsa-miR-15a-5p was downregulated in GC ($P < 0.005$) (Figure 2(g)).

In summary, ONECUT2 is related to the stage, metastasis and grade of GC, and its expression is inversely proportional to the differentiation degree of adenocarcinoma. Secondly, gastric tumor suppressor hsa-miR-15a-5p can target ONECUT2.

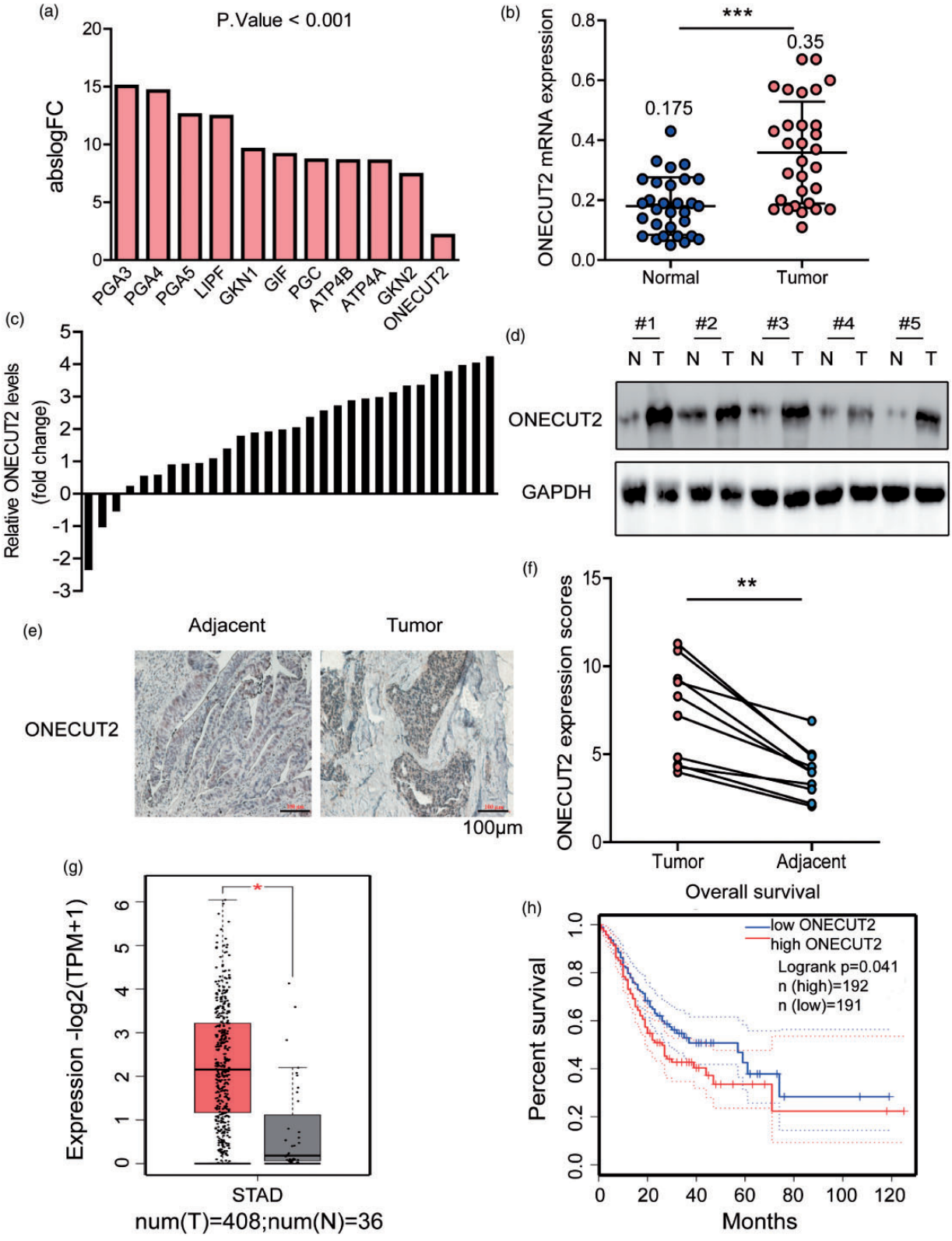

Figure 1. ONECUT2 is an oncogene in gastric cancer. (a) LIMMA R package was used for analyzing differential gene expression of STAD samples and adjacent normal tissues in TCGA Database. ONECUT2 and DEGs whose absLogFC ranked top 10 were exhibited in a histogram. *P* value < 0.001. (b) qPCR analysis of hsa-miR-15a-5p expression between STAD samples and adjacent normal tissues. (c, d) Hsa-miR-15a-5p expression in 30 pairs of STAD samples and their corresponding non-tumorous tissues. (e, f) Immunohistochemistry detected the expression and distribution of ONECUT2 in the STAD samples and adjacent normal tissues and photos were taken. (g, h) GEPIA website analyzed the correlation between ONECUT2 expression and the survival of STAD patients. (A color version of this figure is available in the online journal.)

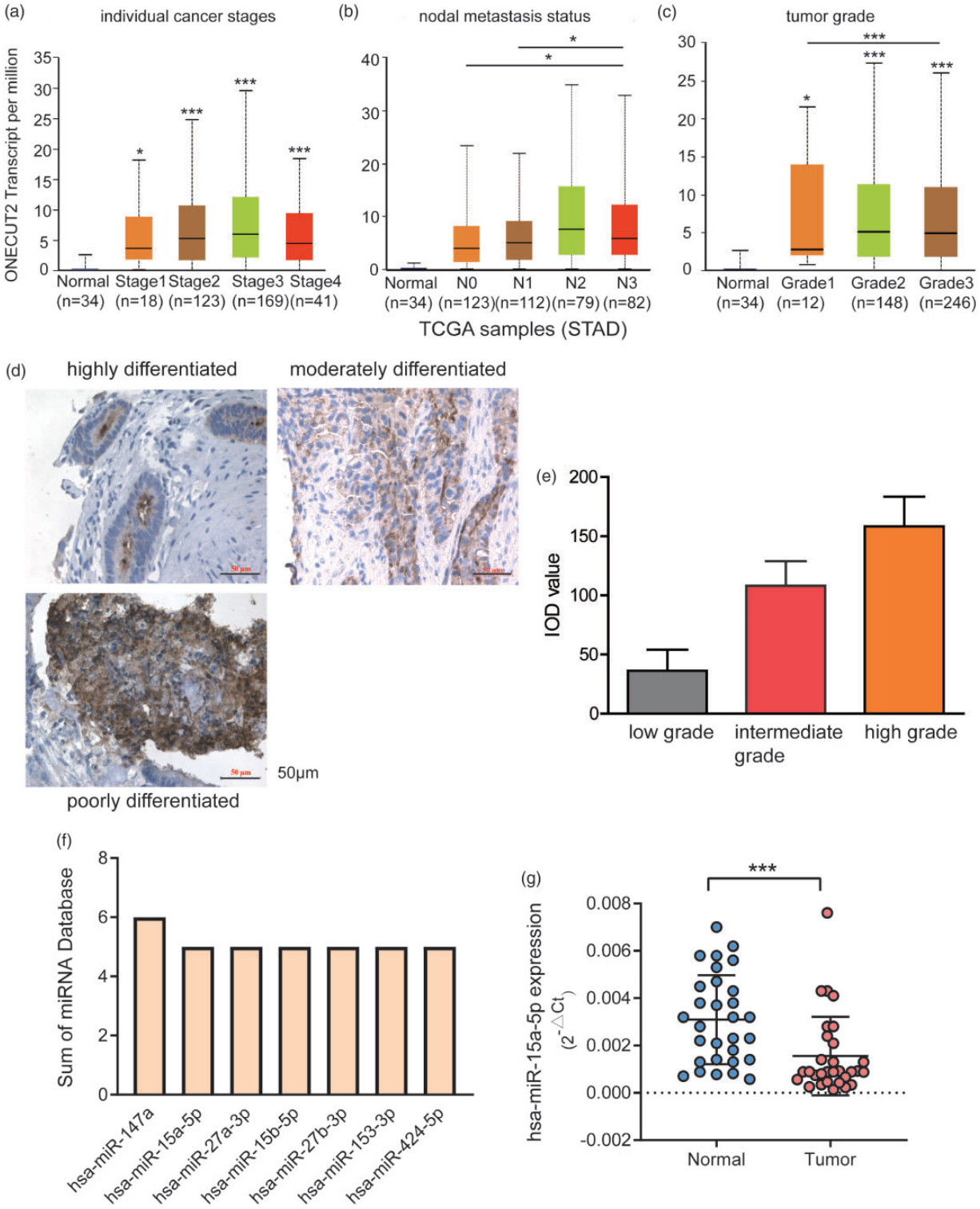

Figure 2. ONECUT2 is inversely proportional to the differentiation degree of gastric cancer tissue. (a–c) UALCAN website analyzed the correlation between ONECUT2 expression and STAD stage, grade and metastasis (N0: no regional lymph node; N1: metatases in 1 to 3 axiliary lymph node; N2: metatases in 4 to 9 axiliary lymph node; N3: metatases in 10 or more axiliary lymph node. Grade 1: well differentiated tissues; Grade 2: moderately differentiated tissues; Grade 3: poorly differentiated tissues; Grade 4: undifferentiated tissues). (d, e) Immunohistochemistry detected the expression of ONECUT2 in GC with distinct differentiation degree. (f) Seven miRNA prediction websites (PITA, RNA22, miRmap, microT, miRanda, PicTar, TargetScan) predicted miRNAs that could regulate ONECUT2. (g) qPCR analysis of hsa-miR-15a-5p expression between STAD samples and adjacent normal tissues. (A color version of this figure is available in the online journal.)

Sorting and identification of gastric cancer stem cells

The first recognition of gastric CSCs was through a heterogeneous lineage of CD44+ subpopulation.[22] Many studies have demonstrated that GCSCs feature increased levels of CD133, CD44, GLI1, SOX2, OCT4, p-ERK, and p-AKT.[23,24] To explore whether hsa-miR-15a-5p can regulate the stemness of GC cells by targeting ONECUT2, we first sorted CD133+/CD44+ MKN45 by fluorescence activated cell sorting (FACS) (Figure 3(a)). qPCR results indicated that, compared with parental MKN45, the stemness-related genes OCT4, SOX2, and nanog all showed significantly higher expression in CD133+/CD44+ MKN45 ($P < 0.05$). The expression of these genes in CD133-/CD44- MKN45 was slightly down-regulated ($P < 0.01$) (Figure 3(b)).

Next, the results of 3-(4,5-dimethylthiazol-2-yl)-2,5-diphenyltetrazolium bromide (MTT) showed that compared with parental MKN45, CD133+/CD44+ MKN45 was less sensitive to traditional GC chemotherapy drugs such as 5-Fu, DDP, and VCR, and presented a multi-drug resistance (MDR) phenotype (Figure 3(c)). Then, colony formation assay experiment indicated that after two weeks, compared with parental and CD133-/CD44- MKN45, CD133+/CD44+ MKN45 presented stronger proliferation ability ($P < 0.001$) (Figure 3(d) and (e)).

In summary, CD133+/CD44+ MKN45 isolated by the surface markers CD133 and CD44 possess stem cell characteristics.

Hsa-miR-15a-5p regulates the transcription and translation of ONECUT2 in GCSCs

To explore whether hsa-miR-15a-5p can regulate the stemness of GC cells by targeting ONECUT2, we have separated CD133+/CD44+ MKN45 by flow cytometry. CD133 and CD44 are two classical markers for gastric CSCs. Double-positive cells are CD133+/CD44+ MKN45 and double-negative cells are CD133-/CD44- MKN45. First, we detected the expression levels of hsa-miR-15a-5p and ONECUT2 in human gastric adenocarcinoma cell lines HGC-27, AGS, SGC-7901, MKN45, and normal human gastric mucosal epithelial cell line GES-1. The results showed that compared with GES-1, hsa-miR-15a-5p was under-expressed in MKN45 ($P < 0.001$) (Figure 4(a)); ONECUT2 was highly expressed in AGS, SGC7901, and MKN45, so we chose MKN45 for flow cytometry sorting. Next, we detected the expression levels of the hsa-miR-15a-5p and ONECUT2 in parental MKN45, CD133+/CD44+ MKN45, and CD133-/CD44- MKN45. qPCR and Western blot results showed that, compared with parental MKN45, the level of hsa-miR-15a-5p was higher in CD133-/CD44- cells and lower in CD133+/CD44+ cells ($P < 0.01$), while ONCUT2 was lower in CD133-/CD44- cells ($P < 0.001$) and higher in CD133+/CD44+ cells ($P < 0.001$), which indicates ONECUT2 is related to stemness maintenance or cell differentiation of GCSC (Figure 4(b) and (c)).

In addition, overexpression of hsa-miR-15a-5p in CD133+/CD44+ cells can inhibit the expression of ONECUT2; inhibition of hsa-miR-15a-5p in CD133-/CD44- cells can promote the expression of ONECUT2, which indicates that hsa-miR-15a-5p can regulate the protein level of ONECUT2 in GCSCs (Figure 4(d)). Then, we searched for the conserved binding site of hsa-miR-15a-5p in the 3′UTR region of ONECUT2 on TargetScan. The dual luciferase reporter gene experiment proved that hsa-miR-15a-5p inhibited the transcription level of ONECUT2 by conservatively binding the "AUCAUC" fragment of the ONECUT2 3′UTR (Figure 4(e) and (f)). To explore the molecular mechanism of ONECUT2 regulating the biological behavior of GCSCs, we constructed ONECUT2 OE. qPCR and Western blot results indicated that the overexpression plasmid was successfully constructed (Figure 4(g) and (h)).

Hsa-miR-15a-5p inhibits GCSC stemness and EMT by targeting ONECUT2

MiRNA is involved in the control of CSC function and can inhibit CSC-specific genes and phenotypes, including self-renewal and tumorigenicity. ONECUT-2 could promote EMT in colorectal and hepatocellular carcinoma, thus promoting tumor invasion and distant metastasis.[14,15] First, the results of stem cell sphere formation assay demonstrated that overexpression of hsa-miR-15a-5p could significantly inhibit the proliferation of GCSCs, that is, simultaneously inhibit the number and diameter of GCSCs spheres ($P < 0.5$). Overexpression of ONECUT2 could significantly weaken the inhibitive effect of hsa-miR-15a-5p on the proliferation of GCSCs (Figure 5(a) to (c)). In order to further explore the influence of hsa-miR-15a-5p and ONECUT2 on stemness maintenance of GCSCs, qRT-PCR and Western blot analyzed the expression levels of stemness-related transcription factors KLF4, CD44, OCT4, and EMT markers E-cadherin, Vimentin, N-cadherin. The results manifested that overexpression of hsa-miR-15a-5p could significantly inhibit the mRNA and protein levels of CD44, OCT4, N-cadherin, and increase the mRNA and protein levels of E-cadherin. In addition, overexpression of ONECUT2 could significantly promote KLF4, OCT4, Vimentin, N-cadherin and inhibit E-cadherin at both mRNA and protein levels (Figure 4(d) and (g)).

Hsa-miR-15a-5p promotes GCSCs drug sensitivity and inhibits tumorigenicity in vivo by targeting ONECUT2

First, MTT experiment evaluated the impact of hsa-miR-15a-5p and ONECUT2 on GCSC drug resistance. The results manifested that overexpression of hsa-miR-15a-5p could significantly promote the sensitivity of CSC to 5-FU and DDP. Overexpression of ONECUT2 could obviously reverse the promoting impact of hsa-miR-15a-5p on drug sensitivity (Figure 6(a) and (b)). Then, the results of *in vitro* limiting dilution assay showed that overexpression of ONECUT2 in CD133+/CD44+ MKN45 reversed the inhibitory effect of hsa-miR-15a-5p on GCSC self-renewal ability, indicating that ONECUT2 is related to maintaining the stemness of GCSC (Figure 6(c)). For the *in vivo* limiting dilution experiment, we first constructed CD133+/CD44+ MKN45 that stably overexpress ONECUT2. The results demonstrated that overexpression of hsa-miR-15a-5p could significantly suppress the tumorigenicity of

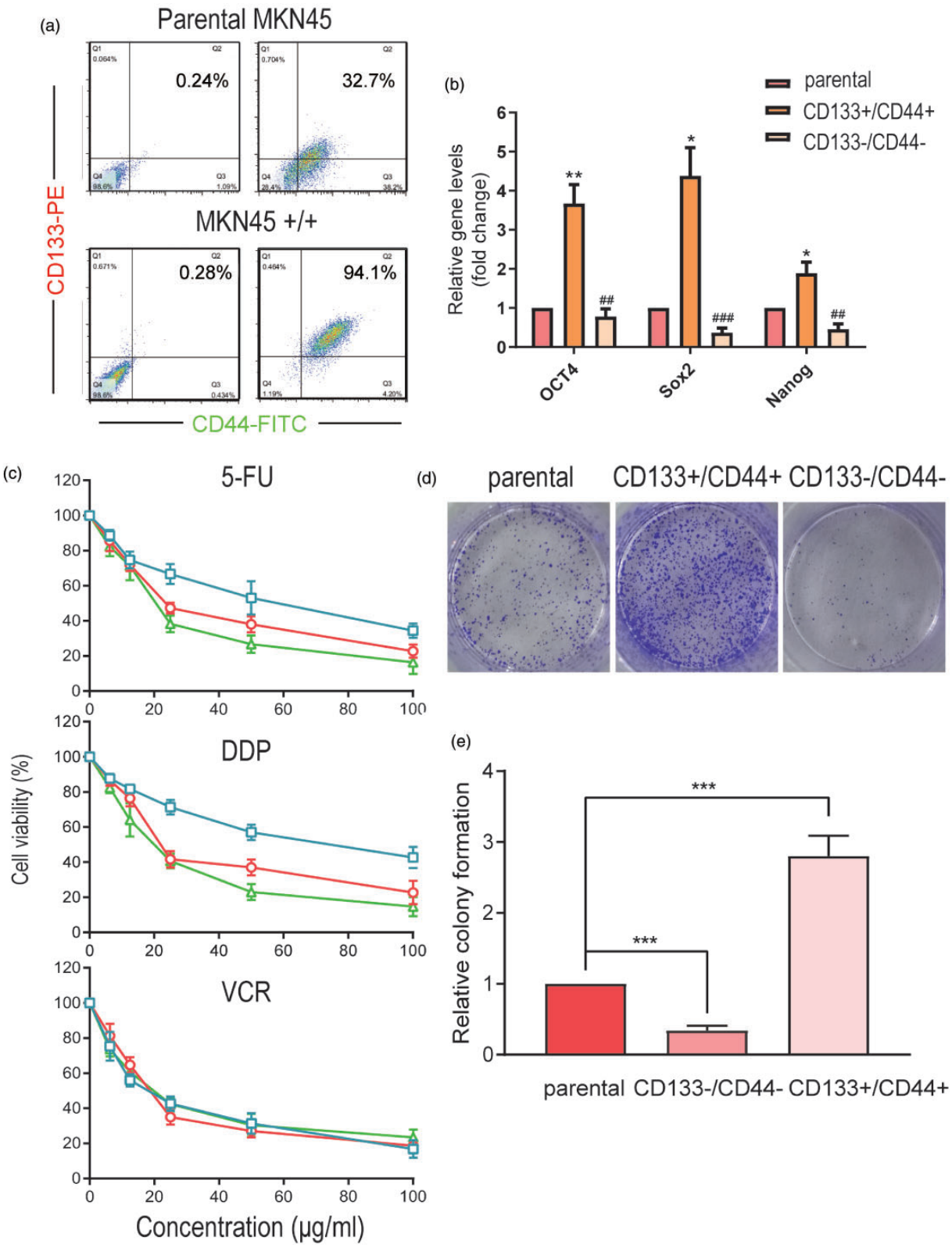

Figure 3. Sorting and identification of gastric cancer stem cells. (a) Sorting gastric cancer stem cells by flow cytometry. Purity of CD133+/CD44+ MNK48 was over 90%. (b) qPCR detected the levels of stemness-associated genes OCT4, Sox2, Nanog. $^{*}P<0.05$, $^{**}P<0.01$, $^{\#\#}P<0.01$, $^{\#\#\#}P<0.001$, ~ versus parental MKN45. (c) MTT detected multi-drug resistance phenotype of parental, CD133-/CD44- and CD133+/CD44+ MKN45 (DDP: cisplatin; VCR: vincristine). (d) Colony forming assay detected the proliferation ability of cells and photos were taken at 14th day. Data were shown as mean±SD. Results comparing two groups were analyzed using Student's *t* test. (A color version of this figure is available in the online journal.)

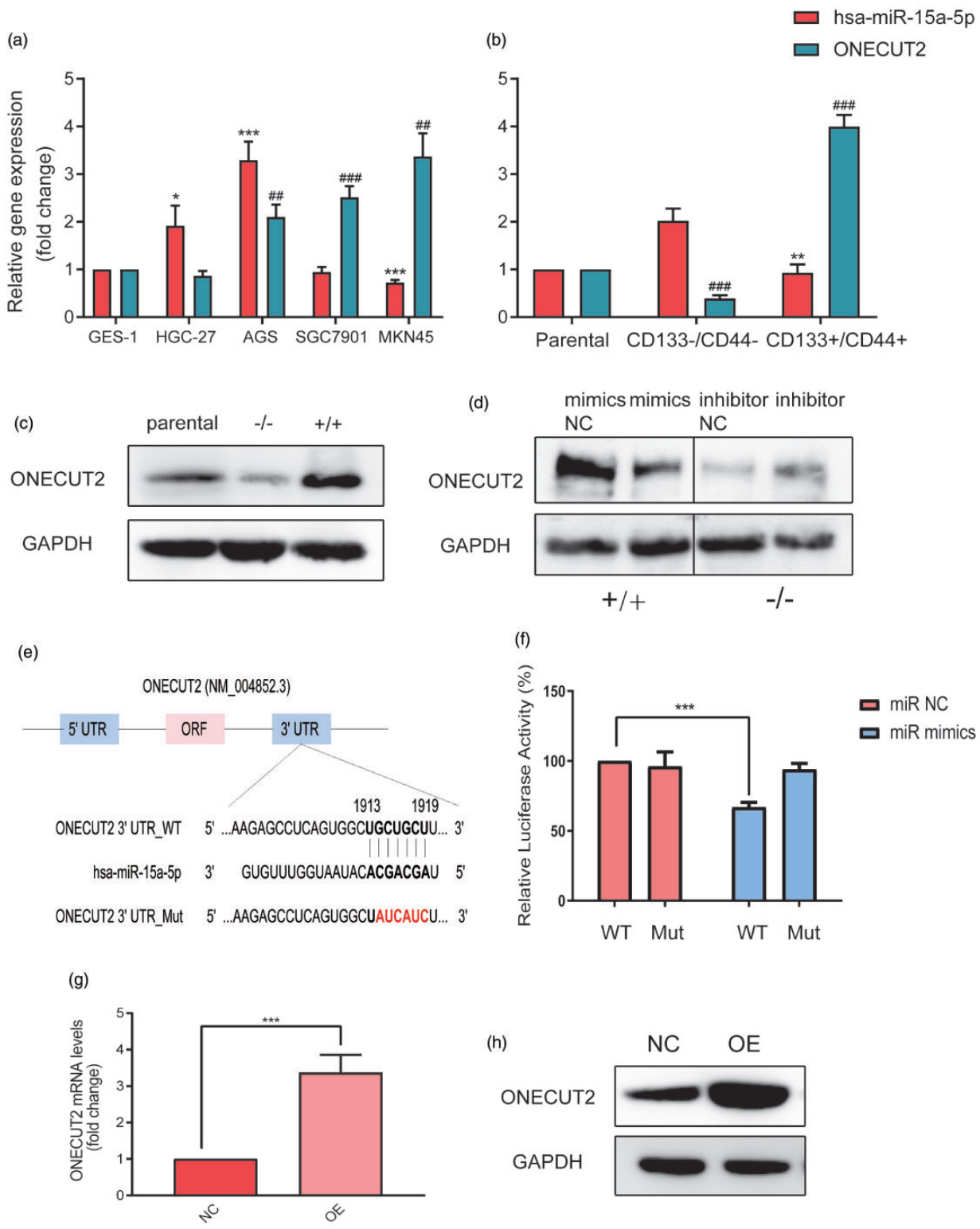

Figure 4. Hsa-miR-15a-5p regulates the transcription and translation of ONECUT2 in GCSCs. (a) qPCR analysis of hsa-miR-15a-5p and ONECUT2 in human gastric adenocarcinoma cell lines HGC-27, AGS, SGC-7901, MKN45 and normal human gastric mucosal epithelial cell line GES-1. $^{*}P<0.05$, $^{***}P<0.001$, $^{\#\#}P<0.01$, $^{\#\#\#}P<0.001$, ~ versus GES-1. (b) qPCR analysis of hsa-miR-15a-5p and ONECUT2 in parental, CD133+/CD44+ and CD133-/CD44- MKN45. $^{**}P<0.01$, $^{\#\#\#}P<0.001$, ~ versus parental MKN45. (c) Western blot detected ONECUT2 expression in parental, CD133+/CD44+ and CD133-/CD44- MKN45. (d) Western blot detected ONECUT2 expression in CD133+/CD44+ MKN45 transfected with hsa-miR-15a-5p mimics, and in CD133-/CD44- MKN45 transfected with hsa-miR-15a-5p inhibitors. (e) The sequence of hsa-miR-15a-5p and its target ONECUT2. (f) We constructed pGL3-ONECUT2-WT and pGL3-ONECUT2-MUT. Then, CD133+/CD44+ MKN45 were transfected with hsa-miR-15a-5p mimics. (g, h) qPCR and Western blot verified the efficiency of ONECUT2 overexpression (OE) vector. (A color version of this figure is available in the online journal.)

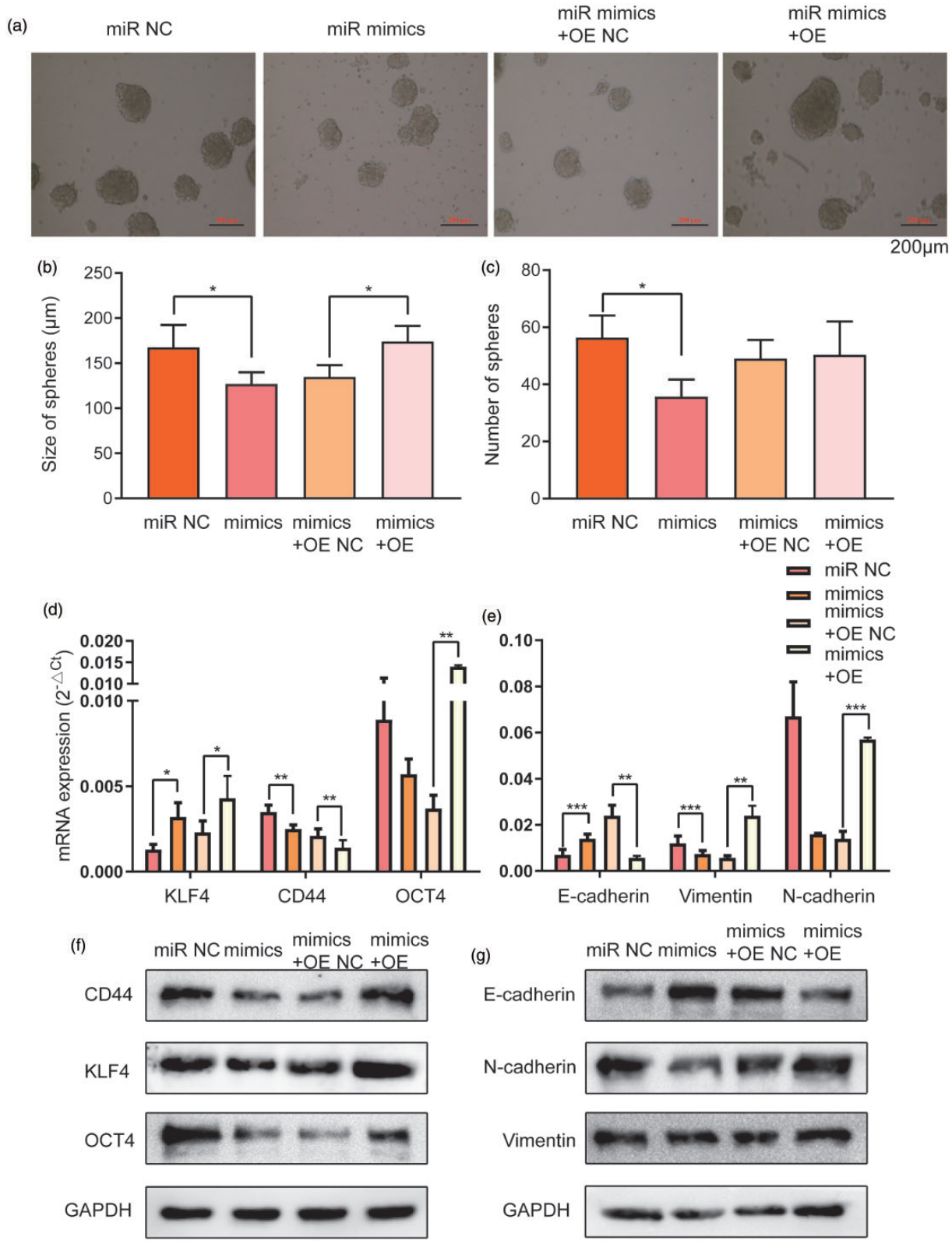

Figure 5. Hsa-miR-15a-5p inhibits GCSC stemness and EMT by targeting ONECUT2. (a–c) Sphere formation assay detected the impacts of hsa-miR-15a-5p mimics or ONECUT2 OE vector on the proliferation of CD133+/CD44+ MKN45. (d, e) qPCR detected the expression levels of stemness-associated genes KLF4, CD44, and OCT4, and EMT marker E-cadherin, Vimentin, and N-cadherin. Data were shown as mean±SD. Results comparing two groups were analyzed using Student's *t* test. (f, g) Western blot analyzed the expression of stemness-associated genes KLF4, CD44, and OCT4, and EMT marker E-cadherin, Vimentin, and N-cadherin in CD133+/CD44+ MKN45. (A color version of this figure is available in the online journal.)

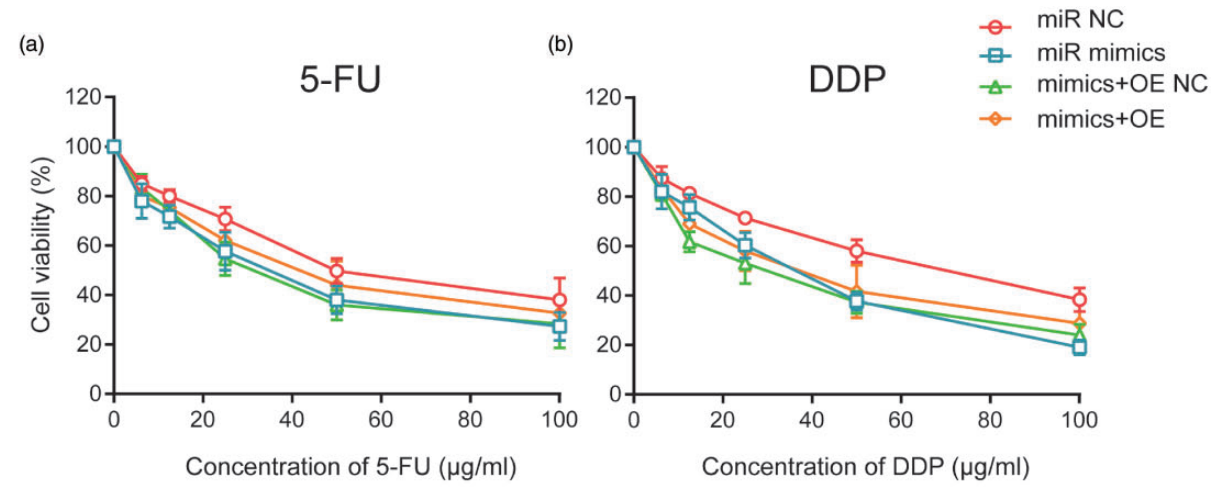

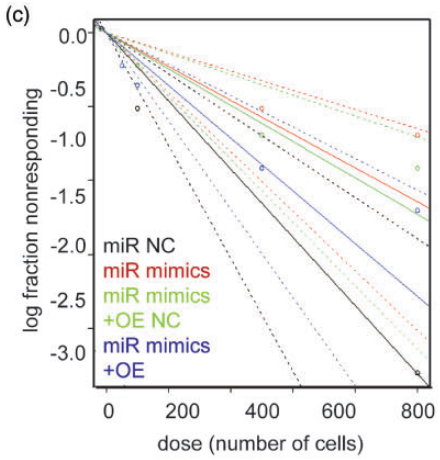

Group	Lower	Estimate	Upper
miR NC	7164	4331	2618
miR mimics	15391	8740	4963
miR mimics +OE NC	14189	8141	4671
miR mimics +OE	9386	5603	3345

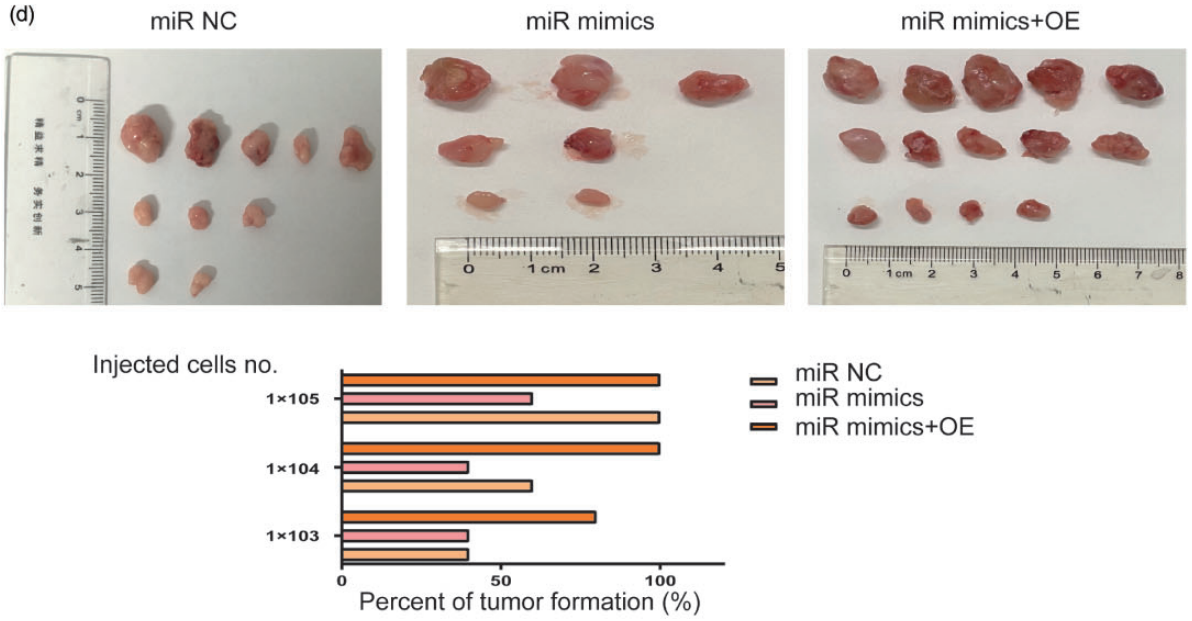

Figure 6. Hsa-miR-15a-5p promotes GCSCs drug sensitivity and inhibits tumorigenicity *in vivo* by targeting ONECUT2. (a, b) MTT detected multi-drug resistance phenotype of CD133+/CD44+ MKN45 transfected with hsa-miR-15a-5p mimics or ONECUT2 OE vector. (c) *In vitro* limiting dilution assay assessed the impacts of hsa-miR-15a-5p mimics or ONECUT2 OE vector on the self-renewal ability of CD133+/CD44+ MKN45. $P<0.001$. (d) *In vivo* limiting dilution assay analyzed the effects of hsa-miR-15a-5p mimics or ONECUT2 OE vector on tumorigenic ability in Balb/c nude mice. Groups: miRNA negative control (2×10^3); hsa-miR-15a-5p mimics (2×10^3); hsa-miR-15a-5p mimics+pEGFP_E2-2 (2×10^3); miRNA negative control (2×10^4); hsa-miR-15a-5p mimics (2×10^4); hsa-miR-15a-5p mimics+pEGFP_E2-2 (2×10^4); miRNA negative control (2×10^5); hsa-miR-15a-5p mimics (2×10^5); hsa-miR-15a-5p mimics+pEGFP_E2-2 (2×10^5). (A color version of this figure is available in the online journal.)

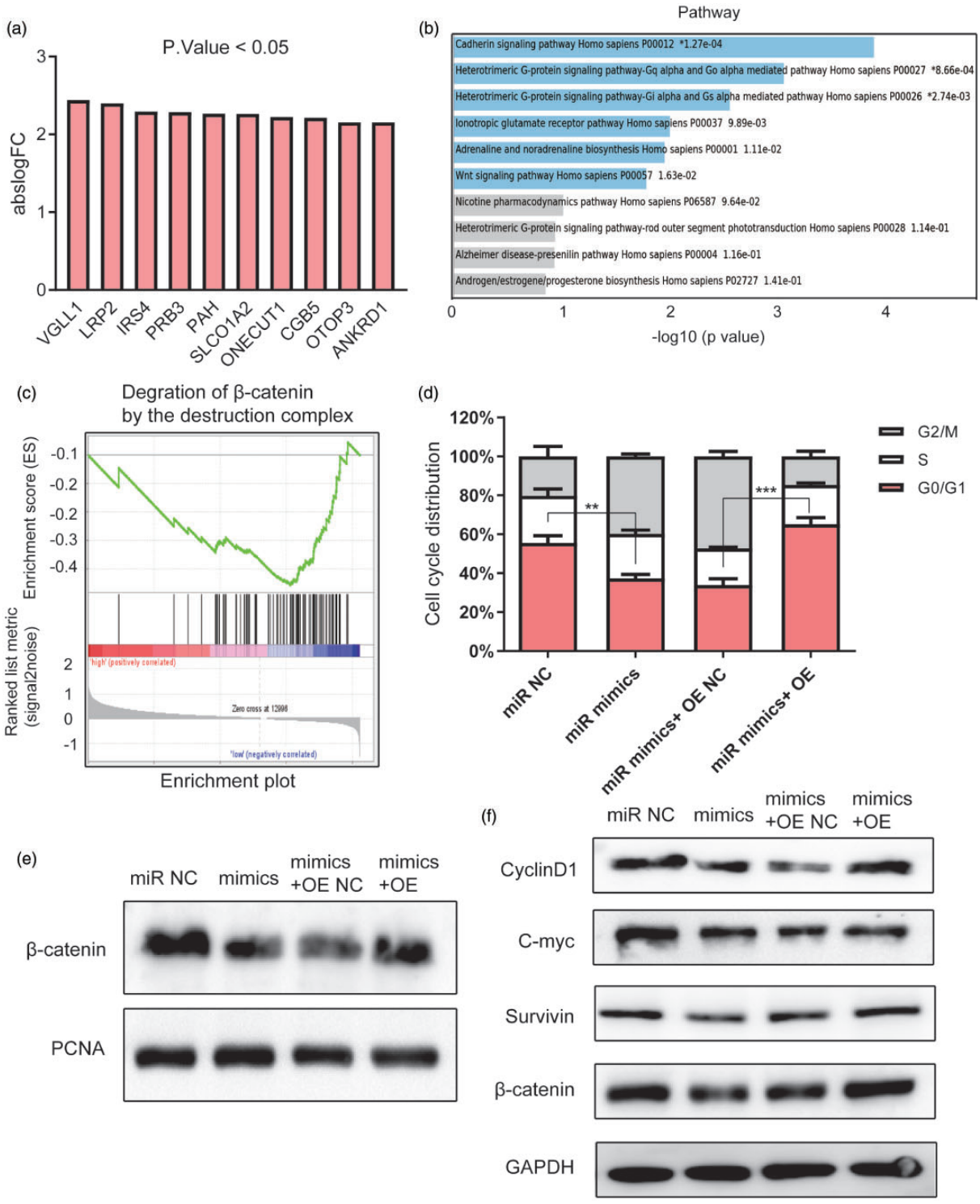

Figure 7. Wnt/β-catenin is the downstream signaling pathway of ONECUT2 in GCSCs. (a) Gastric cancer patients in TCGA Database were divided into high- and low-expression groups. DEGs whose absLogFC ranked top 10 were exhibited in a histogram. (b) Enrichr database performed KEGG pathway enrichment analysis for DEGs. (c) GSEA analysis demonstrated that ONECUT2 has a significant correlation with β-catenin signaling pathway. (d) Flow cytometry detected the effects of hsa-miR-15a-5p mimics or ONECUT2 OE vector on the cell cycle of CD133+/CD44+ MKN45. (e) Western blot detected the expression levels of β-catenin in nucleus. (f) Western blot analyzed the levels of downstream effectors of Wnt/β-catenin in the whole cell protein lysate. (A color version of this figure is available in the online journal.)

CD133+/CD44+ MKN45 *in vivo*, and overexpression of ONECUT2 could apparently enhance the tumorigenicity of CD133+/CD44+ MKN45 *in vivo*, indicating that ONECUT2 promotes tumor initiation ability of CSC *in vivo* (Figure 6(d)).

Wnt/β-catenin is the downstream signaling pathway of ONECUT2 in GCSCs

To screen the signaling pathways regulated by ONECUT2 in GC, GC patients in TCGA Database were divided into

ONECUT2-high and ONECUT2-low expression groups separately. We analyzed DEGs in the two groups. DEGs whose absLogFC ranked top 10 were exhibited (Figure 7 (a)). Then, we utilized Enrichr database (https://maayanlab.cloud/Enrichr/) to perform KEGG pathway enrichment analysis for DEGs (Figure 7(b)). We found that the signaling pathways enriched by DEGs are cadherin signaling pathway, lonotropic glutamate receptor pathway, Wnt signaling pathway, adrenaline and noradrenaline biosynthesis, etc.

Next, we analyzed with GSEA software and discovered that ONECUT2 has a significant correlation with β-catenin signaling pathway (Figure 7(c)). In addition, we also tested the effect of overexpression of hsa-miR-15a-5p and ONECUT2 on the cell cycle of GCSCs. The results proved that overexpression of hsa-miR-15a-5p could obviously reduce the ratio of cells in G0/G1 phase, while overexpression of ONECUT2 could significantly promote the percentage of cells in G0/G1 phase and decrease the percentage of cells in G2/M phase (Figure 7(d)). Then, Western blot results verified that overexpression of hsa-miR-15a-5p could significantly inhibit the expression of β-catenin in the nucleus (Figure 7(e)), and Wnt/β-catenin downstream effectors CyclinD1, C-myc, and Survivin. Overexpression of ONECUT2 could apparently enhance the expression of β-catenin in the nucleus, and intracellular CyclinD1 and Survivin (Figure 7(f)).

In summary, hsa-miR-15a-5p inhibits the block of G0 phase by regulating ONECUT2/β-catenin signaling pathway in GCSCs.

Discussion

Many CSC markers including CD133, CD44, receptor tyrosine kinase, ALDH, EpCAM/ESA, and ABCG2 are effective markers for CSC population in solid tumors.[25] In this study, we sorted CD133+/CD44+ MKN45 by fluorescence activated cell sorting and identified the stem cell phenotype of CD133+/CD44+ cells *in vitro* (Figure 3).

ONECUT2 is a member of ONECUT family of transcription factors, which is involved in proliferation, angiogenesis, EMT, migration, and invasion of cancer cells.[26] Bray *et al*. has shown that ONECUT2 promotes GC cells proliferation through inducing ROCK1 expression at DNA level.[2] Besides, CpGs in the promoter-proximal DNA of ONECUT2 were hypomethylated in GC, which was correlated with up-regulation of ONECUT2.[27] The promoter of ONECUT2 is marked by both K4me3 and K27me3 in embryonic stem cells. This is a pattern called bivalent domain that can silence developmental genes. The bivalent domain is related to the gene encoding of transcription factors related to embryonic development and lineage differentiation. The chromatin regions that exhibit bivalence, including the ONECUT2 promoter, are the main promoters that plays a role in promoting gastric adenocarcinoma. However, miRNAs can be used to reprogram the levels of ONECUT2 and other bivalent genes.[17]

MicroRNAs are potential clinical tools for cancer diagnosis and treatment. Since miRNAs are not digested by endogenous ribonuclease, their levels in plasma and feces are detectable. MiRNA therapy is also a new strategy for cancer therapy. MiRNA reduces the proportion of CSC population by inhibiting CSC functional genes. Several effective delivery systems have been developed for improving anti-cancer treatments. For example, in CSC-induced glioblastoma, polyurethane-polyethyleneimine (PU-PEI)/miR-145 NPs has a good therapeutic effect. Similarly, the delivery of PU-PEI/miR-145 could suppress the stemness of lung CSC, tumor growth, and metastasis *in vivo*.[28] In this project, we confirmed that hsa-miR-15a-5p could regulate the sphere formation, tumorigenicity, and EMT of CD133+/CD44+ MKN45 by regulating ONECUT2. We also discovered that overexpression of ONECUT2 in CD133+/CD44+ MKN45 can promote the sensitivity of CSC to 5-FU and DDP.

Most anti-tumor drugs kill tumor cells by interfering with DNA replication and causing DNA damage. Antitumor drugs mostly target tumor cells that divide rapidly and continue replicating their DNA. However, most CSCs are in a dormant state, which is the G0 phase (rest phase) of DNA replication. In addition, KEGG analysis in a previous study has revealed overexpression of ONECUT2 activated Wnt signaling pathway and cell cycle pathway.[2] Besides, overactivation of the canonical Wnt pathway exists in 30–50% of GC tissues.[29,30] However, it remains unknown whether ONECUT2 are engaged in the cell cycle regulation by modulating Wnt/β-catenin pathway in GC. Our Western blot results manifested that overexpression of hsa-miR-15a-5p could significantly suppress the expression of β-catenin in the nucleus and Wnt/β-catenin downstream effectors, while overexpression of ONECUT2 could apparently enhance the expression of β-catenin in the nucleus (Figure 7), indicating that hsa-miR-15a-5p suppressed the block of G0 phase by regulating ONECUT2/β-catenin signaling pathway in GCSCs.

To conclude, we investigated the clinical significance of hsa-miR-15a-5p and ONECUT2 in GC, and cast new insights into the mechanism underlying hsa-miR-15a-5p and ONECUT2 regulation of GCSC stemness maintenance and EMT. However, the clinical application of hsa-miR-15a-5p and ONECUT2 still requires further investigation.

Conclusions

We could conclude that overexpression of hsa-miR-15a-5p promotes CD133+/CD44+ MKN45 chemosensitivity by inhibiting the expression levels of its target ONECUT2, thus impacting the transcription of Wnt/β-catenin pathway downstream molecules which modulate stemness and EMT phenotype, and ultimately weakens the self-renewal ability of GCSCs.

AUTHORS' CONTRIBUTIONS

CS, WG, and XJZ were involved in the design of the studies; CS and JFW conducted *in vitro* experiments and bioinformatics analysis; LPZ conducted *in vivo* experiment; CS and XJZ analyzed all the data and wrote the manuscript; XJZ approved the submission.

DECLARATION OF CONFLICTING INTERESTS

The author(s) declared no potential conflicts of interest with respect to the research, authorship, and/or publication of this article.

ETHICAL APPROVAL

Thirty cases of human gastric cancer and adjacent normal tissues were collected with ethical approval from the research ethics committees of The First Affiliated Hospital of Soochow University.

FUNDING

The author(s) received no financial support for the research, authorship, and/or publication of this article.

DATA AVAILABILITY

The data that support the findings of this study are available from the corresponding author upon reasonable request.

ORCID iD

Xiaojun Zhou https://orcid.org/0000-0002-9652-4890

Supplemental Material

Supplementary material for this article is available online.

REFERENCES

1. Siegel RL, Miller KD, Jemal A. Cancer statistics, 2020. *CA – Cancer J Clin* 2020;**70**:7–30
2. Bray F, Ferlay J, Soerjomataram I, Siegel RL, Torre LA, Jemal A. Global cancer statistics 2018: GLOBOCAN estimates of incidence and mortality worldwide for 36 cancers in 185 countries. *CA – Cancer J Clin* 2018;**68**:394–424
3. Dewi DL, Ishii H, Kano Y, Nishikawa S, Haraguchi N, Sakai D, Satoh T, Doki Y, Mori M. Cancer stem cell theory in gastrointestinal malignancies: recent progress and upcoming challenges. *J Gastroenterol* 2011;**46**:1145–57
4. Zhang N, Li R, Tao KS, Cao DY, Ti ZY, Ding R, Cai L, Zhang FQ, Dou KF. Characterization of a stem-like population in hepatocellular carcinoma MHCC97 cells. *Oncol Rep* 2010;**23**:827–31
5. Liu T, Xu F, Du X, Lai D, Liu T, Zhao Y, Huang Q, Jiang L, Huang W, Cheng W, Liu Z. Establishment and characterization of multi-drug resistant, prostate carcinoma-initiating stem-like cells from human prostate cancer cell lines 22RV1. *Mol Cell Biochem* 2010;**340**:265–73
6. Sapkota D, Chintala H, Wu F, Fliesler SJ, Hu Z, Mu X. Onecut1 and Onecut2 redundantly regulate early retinal cell fates during development. *Proc Natl Acad Sci U S A* 2014;**111**:E4086–95
7. Klimova L, Antosova B, Kuzelova A, Strnad H, Kozmik Z. Onecut1 and Onecut2 transcription factors operate downstream of Pax6 to regulate horizontal cell development. *Dev Biol* 2015;**402**:48–60
8. Wu Y, Jiang G, Zhang N, Liu S, Lin X, Perschon C, Zheng SL, Ding Q, Wang X, Na R, Sun J, Xu J. HOXA9, PCDH17, POU4F2, and ONECUT2 as a urinary biomarker combination for the detection of bladder cancer in Chinese patients with hematuria. *Eur Urol Focus* 2020;**6**:284–91
9. Lu T, Wu B, Yu Y, Zhu W, Zhang S, Zhang Y, Guo J, Deng N. Blockade of ONECUT2 expression in ovarian cancer inhibited tumor cell proliferation, migration, invasion and angiogenesis. *Cancer Sci* 2018;**109**:2221–34
10. Guo H, Ci X, Ahmed M, Hua JT, Soares F, Lin D, Puca L, Vosoughi A, Xue H, Li E, Su P, Chen S, Nguyen T, Liang Y, Zhang Y, Xu X, Xu J, Sheahan AV, Ba-Alawi W, Zhang S, Mahamud O, Vellanki RN, Gleave M, Bristow RG, Haibe-Kains B, Poirier JT, Rudin CM, Tsao MS, Wouters BG, Fazli L, Feng FY, Ellis L, van der Kwast T, Berlin A, Koritzinsky M, Boutros PC, Zoubeidi A, Beltran H, Wang Y, He HH. ONECUT2 is a driver of neuroendocrine prostate cancer. *Nat Commun* 2019;**10**:278
11. Rotinen M, You S, Yang J, Coetzee SG, Reis-Sobreiro M, Huang WC, Huang F, Pan X, Yáñez A, Hazelett DJ, Chu CY, Steadman K, Morrissey CM, Nelson PS, Corey E, Chung LWK, Freedland SJ, Di Vizio D, Garraway IP, Murali R, Knudsen BS, Freeman MR. ONECUT2 is a targetable master regulator of lethal prostate cancer that suppresses the androgen axis. *Nat Med* 2018;**24**:1887–98
12. Sun Y, Shen S, Liu X, Tang H, Wang Z, Yu Z, Li X, Wu M. MiR-429 inhibits cells growth and invasion and regulates EMT-related marker genes by targeting Onecut2 in colorectal carcinoma. *Mol Cell Biochem* 2014;**390**:19–30
13. Zhang J, Cheng J, Zeng Z, Wang Y, Li X, Xie Q, Jia J, Yan Y, Guo Z, Gao J, Yao M, Chen X, Lu F. Comprehensive profiling of novel microRNA-9 targets and a tumor suppressor role of microRNA-9 via targeting IGF2BP1 in hepatocellular carcinoma. *Oncotarget* 2015;**6**:42040–52
14. Jung SY, Papp JC, Sobel EM, Pellegrini M, Yu H, Zhang ZF. Pro-inflammatory cytokine polymorphisms in ONECUT2 and HNF4A and primary colorectal carcinoma: a post genome-wide gene-lifestyle interaction study. *Am J Cancer Res* 2020;**10**:2955–76
15. Hu J, Chen Y, Li X, Miao H, Li R, Chen D, Wen Z. THUMPD3-AS1 is correlated with non-small cell lung cancer and regulates self-renewal through miR-543 and ONECUT2. *Onco Targets Ther* 2019;**12**:9849–60
16. Shen M, Dong C, Ruan X, Yan W, Cao M, Pizzo D, Wu X, Yang L, Liu L, Ren X, Wang SE. Chemotherapy-induced extracellular vesicle miRNAs promote breast cancer stemness by targeting ONECUT2. *Cancer Res* 2019;**79**:3608–21
17. Liu J, Valencia-Sanchez MA, Hannon GJ, Parker R. MicroRNA-dependent localization of targeted mRNAs to mammalian P-bodies. *Nat Cell Biol* 2005;**7**:719–23
18. Tang Z, Li C, Kang B, Gao G, Li C, Zhang Z. GEPIA: a web server for cancer and normal gene expression profiling and interactive analyses. *Nucleic Acids Res* 2017;**45**:W98–102
19. Chandrashekar DS, Bashel B, Balasubramanya SAH, Creighton CJ, Ponce-Rodriguez I, Chakravarthi B, Varambally S. UALCAN: a portal for facilitating tumor subgroup gene expression and survival analyses. *Neoplasia (New York, NY)* 2017;**19**:649–58
20. Chen EY, Tan CM, Kou Y, Duan Q, Wang Z, Meirelles GV, Clark NR, Ma'ayan A. Enrichr: interactive and collaborative HTML5 gene list enrichment analysis tool. *BMC Bioinformatics* 2013;**14**:128
21. Ma X, Liu J, Li J, Li Y, Le VM, Li S, Liang X, Liu L, Liu J. miR-139-5p reverses stemness maintenance and metastasis of colon cancer stem-like cells by targeting E2-2. *J Cell Physiol* 2019;**234**:22703–18
22. Takaishi S, Okumura T, Tu S, Wang SS, Shibata W, Vigneshwaran R, Gordon SA, Shimada Y, Wang TC. Identification of gastric cancer stem cells using the cell surface marker CD44. *Stem Cells (Dayton, Ohio)* 2009;**27**:1006–20
23. Zhang X, Hua R, Wang X, Huang M, Gan L, Wu Z, Zhang J, Wang H, Cheng Y, Li J, Guo W. Identification of stem-like cells and clinical significance of candidate stem cell markers in gastric cancer. *Oncotarget* 2016;**7**:9815–31
24. Qiao XT, Gumucio DL. Current molecular markers for gastric progenitor cells and gastric cancer stem cells. *J Gastroenterol* 2011;**46**:855–65
25. Shapira A, Livney YD, Broxterman HJ, Assaraf YG. Nanomedicine for targeted cancer therapy: towards the overcoming of drug resistance. *Drug Resist Updat* 2011;**14**:150–63

26. Wang GH, Zhou YM, Yu Z, Deng JP, Liu SF, Wei CZ, Feng Y, Mao M, Wang Z. Up-regulated ONECUT2 and down-regulated SST promote gastric cell migration, invasion, epithelial–mesenchymal transition and tumor growth in gastric cancer. *Eur Rev Med Pharmaco* 2020;**24**:9378–90
27. Seo EH, Kim HJ, Kim JH, Lim B, Park JL, Kim SY, Lee SI, Jeong HY, Song KS, Kim YS. ONECUT2 upregulation is associated with CpG hypomethylation at promoter-proximal DNA in gastric cancer and triggers ACSL5. *Int J Cancer* 2020;**146**:3354–68
28. Yang YP, Chien Y, Chiou GY, Cherng JY, Wang ML, Lo WL, Chang YL, Huang PI, Chen YW, Shih YH, Chen MT, Chiou SH. Inhibition of cancer stem cell-like properties and reduced chemoradioresistance of glioblastoma using microRNA145 with cationic polyurethane-short branch PEI. *Biomaterials* 2012;**33**:1462–76
29. Clements WM, Wang J, Sarnaik A, Kim OJ, MacDonald J, Fenoglio-Preiser C, Groden J, Lowy AM. Beta-catenin mutation is a frequent cause of Wnt pathway activation in gastric cancer. *Cancer Res* 2002;**62**:3503–6
30. Ooi CH, Ivanova T, Wu J, Lee M, Tan IB, Tao J, Ward L, Koo JH, Gopalakrishnan V, Zhu Y, Cheng LL, Lee J, Rha SY, Chung HC, Ganesan K, So J, Soo KC, Lim D, Chan WH, Wong WK, Bowtell D, Yeoh KG, Grabsch H, Boussioutas A, Tan P. Oncogenic pathway combinations predict clinical prognosis in gastric cancer. *PloS Genet* 2009;**5**:e1000676

(Received March 4, 2021, Accepted July 11, 2021)